The Canadian Mineralogist
Vol. 47, pp. 193-204 (2009)
DOI: 10.3749/canmin.47.1.193

BUSSYITE-(Ce), A NEW BERYLLIUM SILICATE MINERAL SPECIES FROM MONT SAINT-HILAIRE, QUEBEC

JOEL D. GRICE§, RALPH ROWE AND GLENN POIRIER

Research Division, Canadian Museum of Nature, P.O. Box 3443, Station D, Ottawa, Ontario K1P 6P4, Canada

ALLEN PRATT

CANMET, Mining and Mineral Sciences Laboratories, 555 Booth Street, Ottawa, Ontario K1A 0G1, Canada

JAMES FRANCIS

Surface Science Western, University Western Ontario, London, Ontario N6A 5B7, Canada

ABSTRACT

Bussyite-(Ce), ideally $(Ce,REE,Ca)_3(Na,H_2O)_6MnSi_9Be_5(O,OH)_{30}(F,OH)_4$, a new mineral species, was found in the Mont Saint-Hilaire quarry, Quebec. The crystals are transparent to translucent, pale pinkish orange in color, with a white streak and vitreous luster. Bladed crystals are prismatic, having forms $\{11\bar{1}\}$ and $\{10\bar{1}\}$; they are elongate on [101], up to 10 mm in length. Associated minerals include aegirine, albite, analcime, ancylite-(Ce), calcite, catapleiite, gonnardite, hydrotalcite, kupletskite, leucophanite, microcline, nenadkevichite, polylithionite, serandite and sphalerite. Bussyite-(Ce) is monoclinic, space group *C*2/*c*, with unit-cell parameters refined from powder-diffraction data: *a* 11.654(3), *b* 13.916(3), *c* 16.583(4) Å, β 95.86(2)°, *V* 2675.4(8) Å^3 and *Z* = 4. Electron-microprobe and secondary-ion mass spectrometric analyses give the average and ranges: Na_2O 7.63 (9.40–6.62), K_2O 0.05 (0.13–0.0), BeO 8.33 (SIMS), CaO 5.35 (5.95–4.17), MgO 0.03 (0.11–0.00), MnO 2.49 (3.00–1.71), Al_2O_3 0.82 (1.54–0.39), Y_2O_3 1.97 (2.68–1.51), La_2O_3 2.65 (3.11–2.16), Ce_2O_3 9.77 (11.22 –8.15), Pr_2O_3 1.23 (1.49 –0.74), Nd_2O_3 4.54 (5.13–3.91), Sm_2O_3 0.99 (1.25–0.68), Eu_2O_3 0.010 (0.25–0.0), Gd_2O_3 1.03 (1.23–0.81), SiO_2 38.66 (39.94–37.66), ThO_2 3.31 (4.59–2.12), F 3.67 (6.39–2.54), S 0.03 (0.08–0), H_2O 4.12 (determined from crystal-structure analysis), for a total of 95.21 wt.%. The empirical formula based on the crystal-structure analysis, ideally showing 34 anions, is: $4\{(Ce_{0.823}Nd_{0.373}Y_{0.242}Th_{0.173}Pr_{0.103}Sm_{0.079}Gd_{0.078}Eu_{0.008})_{\Sigma 1.879}(Ca_{0.775}La_{0.225})_{\Sigma 1}[Na_{3.000}(H_2O)_{\Sigma 2.500}Ca_{0.544}K_{0.015}]_{\Sigma 6.055}(Mn_{0.485}Na_{0.402}Mg_{0.012})_{\Sigma 0.899}(Si_{8.897}Be_{4.605}Al_{0.222})_{\Sigma 13.724}O_{30}[F_{2.67}(OH)_{1.33}]_{\Sigma 4}\}$. The structure has been refined to an *R* index of 4.0% for 1134 unique, observed reflections. The structure has two chemically distinct layers parallel to $(10\bar{1})$: (1) a layer of $[(Si,Be)O_4]$ tetrahedra, and (2) a layer of Ce–, Ca–, Mn–, Na–(O,F) polyhedra. Layers are cross-linked through shared O and F atoms. Significant amounts of OH and H_2O are present, as indicated in the IR spectrum and crystal-structure analysis for the Na-poor hydrated phase. One instance of a rarer Na-rich phase is observed. Based on the electron-microprobe data, the formula for the rarer Na-rich anhydrous phase is $4\{(Ce_{1.047}Nd_{0.466}La_{0.323}Y_{0.306}Pr_{0.131}Sm_{0.102}Gd_{0.084}Eu_{0.009}Th_{0.042})_{\Sigma 2.510}(Na_{6.645}Ca_{0.701})_{\Sigma 7.346}(Si_{9.521}Be_{4.772})_{\Sigma 14.293}O_{29.251}F_{4.749}\}$. Comparing the structure of bussyite-(Ce) to that of other beryllium silicates, the topology of the layer of tetrahedra most strongly resembles that of semenovite-(Ce) and the closely related mineral harstigite.

Keywords: bussyite-(Ce), new mineral species, crystal structure, rare-earth elements, beryllium, infrared spectroscopy, hydrogen, Mont Saint-Hilaire, Quebec.

SOMMAIRE

La bussyite-(Ce), de composition idéale $(Ce,TR,Ca)_3(Na,H_2O)_6MnSi_9Be_5(O,OH)_{30}(F,OH)_4$, est une nouvelle espèce minérale découverte à la carrière du mont Saint-Hilaire, Québec. Les cristaux sont transparents à translucides, d'une couleur orange rosâtre pâle, avec une rayure blanche et un éclat vitreux. Les cristaux lamellaires sont prismatiques, avec les formes $\{11\bar{1}\}$ et $\{10\bar{1}\}$; ils sont allongés sur [101], et atteignent une longueur de 10 mm. Lui sont associés aegirine, albite, analcime, ancylite-(Ce), calcite, catapléiite, gonnardite, hydrotalcite, kupletskite, leucophanite, microcline, nenadkevichite, polylithionite, serandite et sphalérite. La bussyite-(Ce) est monoclinique, groupe spatial *C*2/*c*, avec les paramètres réticulaires suivants, affinés à partir des données obtenues sur poudre: *a* 11.654(3), *b* 13.916(3), *c* 16.583(4) Å, β 95.86(2)°, *V* 2675.4(8) Å^3 et *Z* = 4. Les analyses effectuées avec une microsonde électronique et par spectrométrie de masse des ions secondaires ont donné la moyenne et les

§ *E-mail address*: jgrice@mus-nature.ca

intervalles de valeurs suivants: Na_2O 7.63 (9.40–6.62), K_2O 0.05 (0.13–0.0), BeO 8.33 (SIMS), CaO 5.35 (5.95–4.17), MgO 0.03 (0.11–0.00), MnO 2.49 (3.00–1.71), Al_2O_3 0.82 (1.54–0.39), Y_2O_3 1.97 (2.68–1.51), La_2O_3 2.65 (3.11–2.16), Ce_2O_3 9.77 (11.22 –8.15), Pr_2O_3 1.23 (1.49 –0.74), Nd_2O_3 4.54 (5.13–3.91), Sm_2O_3 0.99 (1.25–0.68), Eu_2O_3 0.010 (0.25–0.0), Gd_2O_3 1.03 (1.23–0.81), SiO_2 38.66 (39.94–37.66), ThO_2 3.31 (4.59–2.12), F 3.67 (6.39–2.54), S 0.03 (0.08–0), H_2O 4.12 (déterminé à partir de l'ébauche de la structure), pour un total de 95.21% (poids). La formule empirique fondée sur les résultats de l'analyse structurale, contenant de façon idéale 34 anions, est: $4\{(Ce_{0.823}Nd_{0.373}Y_{0.242}Th_{0.173}Pr_{0.103}Sm_{0.079}Gd_{0.078}Eu_{0.008})_{\Sigma 1.879}\ (Ca_{0.775}La_{0.225})_{\Sigma 1}\ [Na_{3.000}(H_2O)_{\Sigma 2.500}Ca_{0.544}K_{0.015}]_{\Sigma 6.055}\ (Mn_{0.485}Na_{0.402}Mg_{0.012})_{\Sigma 0.899}\ (Si_{8.897}Be_{4.605}Al_{0.222})_{\Sigma 13.724}O_{30}[F_{2.67}(OH)_{1.33}]_{\Sigma 4}\}$. Nous avons affiné la structure jusqu'à un résidu *R* de 4.0% en utilisant 1134 réflexions uniques observées. La structure possède deux couches chimiquement distinctes parallèles à $(10\bar{1})$: (1) une couche de tétraèdres $[(Si,Be)O_4]$, et (2) une couche de polyèdres Ce–, Ca–, Mn–, Na–(O,F). Ces couches sont interliées grâce à des atomes de O et de F partagés. Des quantités importantes de OH et H_2O sont présentes, comme l'indiquent le spectre d'absorption infrarouge et l'analyse de la structure cristalline de la phase hydratée à teneur en sodium plus faible. Nous avons décelé dans un cas une phase plus rare enrichie en Na. Les données de microsonde électronique montrent que cette phase anhydre riche en Na serait $4\{(Ce_{1.047}Nd_{0.466}La_{0.323}Y_{0.306}Pr_{0.131}Sm_{0.102}Gd_{0.084}Eu_{0.009}Th_{0.042})_{\Sigma 2.510}\ (Na_{6.645}Ca_{0.701})_{\Sigma 7.346}\ (Si_{9.521}Be_{4.772})_{\Sigma 14.293}O_{29.251}F_{4.749}\}$. D'après une comparaison de la structure de la bussyite-(Ce) à celle d'autres silicates de béryllium, la topologie de la couche de tétraèdres ressemble davantage à celle de la semenovite-(Ce) et de la harstigite, qui lui ressemble structuralement.

(Traduit par la Rédaction)

Mots-clés: bussyite-(Ce), nouvelle espèce minérale, structure cristalline, terres rares, béryllium, spectroscopie infrarouge, hydrogène, mont Saint-Hilaire, Québec.

Introduction

Over the span of many years, Dr. Peter Tarassoff and Mr. Gilles Haineault, avid mineral collectors from Montreal, Quebec, have provided us with numerous samples of "unknowns" from Mont Saint-Hilaire, Quebec. Through their efforts and keen eyes, they have greatly furthered the knowledge about this important geological occurrence. These gentlemen found the present "unknown" (UK118) in August, 2004. It was submitted to the Canadian Museum of Nature for identification in May 2006. The lack of a good match for the X-ray powder-diffraction pattern began the present research project. It is evident from this publication that the proper description of a new, complex mineral requires the cooperation of many laboratories. The "worth" of such efforts is often questioned. We believe that all good science comes from minute, detailed investigations. The benefits of such inquiry are: improved understanding of materials, more complete structural classifications, element behavior in varying crystal-chemical environments, and mineral genesis.

The name *bussyite* honors the French chemist Antoine Alexandre Brutus Bussy (1794–1882). Bussy's main interest was pharmaceuticals, but he researched the preparation of magnesium, and he and Friedrich Wöhler are each credited with independently isolating the element beryllium in August 1828 (Bussy 1828). The new mineral, a beryllium silicate, is one of several silicates of beryllium found in alkaline intrusions. Alkaline intrusions were not included to any extent in the seminal work on the mineralogy, petrology and geochemistry of beryllium (Grew 2002), but this occurrence is the main topic in the recent work of Raade (2008). Alkaline rocks are not an economic source of beryllium, but the element is essential in 37 mineral species occurring in syenitic pegmatites (Raade 2008). Of these, Raade (2008) listed 16 occurring at Mont Saint-Hilaire, and there are an additional three, beryl, beryllonite and bussyite-(Ce). All are listed below in the section on Occurrence. Some of the minerals described are zeolites and warrant research into their exchange properties and application as sieves (Grice 2008).

The description of the new mineral species *bussyite-(Ce)* was plagued by the intimate association of two closely related phases, patches of the rare anhydrous bussyite in a primarily hydrous bussyite. As the crystal structure-analysis was done on a crystal that was primarily, but most probably not entirely, hydrated, we have a composite picture of the mechanism by which hydration occurs. There are several differences in the chemical composition between the two phases, and these differences help unravel the genesis of the new mineral. We recognize that ideally one could propose two different mineral species here, but we regard the two phases as a series for which the only complete dataset we have at present pertains to the hydrous member.

The new mineral and its name have been approved by the Commission on New Minerals, Names and Classification (CNMNC), IMA (IMA #2007–039). The holotype specimen (catalogue #CMNMC 85929) is housed in the collection of the Canadian Museum of Nature, Ottawa.

Occurrence

Bussyite-(Ce) was found in a serandite-bearing pocket, approximately 15 × 30 cm across, in a pegmatite hosted by nepheline syenite with albite phenocrysts. The pocket was located in the southwest face of the Poudrette quarry, level 7, Mont Saint-Hilaire, Rouville

County, Quebec. Associated minerals include aegirine, albite, analcime, ancylite-(Ce), calcite, catapleiite, gonnardite, hydrotalcite, kupletskite, leucophanite, microcline, nenadkevichite, polylithionite, serandite and sphalerite. To date, 19 Be-bearing mineral species have been found at Mont Saint-Hilaire: barylite, bavenite, behoite, beryl, beryllonite, bussyite-(Ce), chkalovite, epididymite, eudidymite, genthelvite, helvite, hingganite-(Ce), hingganite-(Y), leifite, leucophanite, milarite, niveolanite and tugtupite, as well as $KNa_6[Be_2Al_3Si_{15}O_{39}F_2]$ (IMA number 2007–017). Most of these species occur within a pegmatite or closely associated with one.

Physical and Optical Properties

Bussyite-(Ce) belongs to the monoclinic crystal system in the prismatic class, 2/*m*. The crystals are prismatic in habit, bounded by the $\{11\bar{1}\}$ prism and $\{10\bar{1}\}$ pinacoid, and elongate on [101], up to 10 mm in length but generally less than half this length (Fig. 1). In the figure, it is evident that the terminations are not smooth. The rough surface, approximately the (101) plane, will be explained in the section on Description of the Structure. The crystals are transparent to translucent, pale pinkish orange in color, with a white streak and vitreous luster. There is no fluorescence in either short-wave or long-wave ultraviolet light. Bussyite-(Ce) has an approximate hardness of 4 (Mohs hardness scale), is brittle and splintery, with a perfect $\{10\bar{1}\}$ cleavage. The density of 3.00 g/cm^3, measured by the flotation method, agrees reasonably well with the calculated density of 3.11 g/cm^3.

Bussyite-(Ce) is biaxial negative, α 1.574(2), β 1.591(2), γ 1.597(2), $2V_{meas}$ 63(2)°, $2V_{calc}$ 61°. Dispersion could not be observed, and there is no pleochroism. The optical orientation is $X \wedge \mathbf{c} = 39°$ (β acute), Y = **b**, and $Z \wedge \mathbf{a} = 44.5°$ (β obtuse). Fine, lamellar twinning, parallel to the elongation, was seen in some crystals.

Chemical Composition

Electron-microprobe analysis

Compositions were obtained using a JEOL 733 Superprobe in WDS mode. Beam conditions were 15 kV and 10 (Na and F) or 20 nA (other elements), with a beam diameter of 20 μm. Counts were collected for 25 s or until 0.50% precision was attained. A summary of the results is presented in Table 1. In spite of the high sodium content of this mineral, it proved to be very resistant to beam damage. Monitoring of Na*K*α counts over a period of several minutes (longer than the total duration of the analysis) showed no detectable change in count rate. The following X-ray lines and standards were used for analysis: Na*K*α and Si*K*α: albite, Ca*K*α: diopside, Mg*K*α: enstatite, Mn*K*α: tephroite, Al*K*α and K*K*α: sanidine, La*L*α, Ce*L*α, Pr*L*α, Nd*L*α, Sm*L*α, Eu*K*α and Gd*K*α: synthetic $REEPO_4$; Y*L*α: synthetic yttrium iron garnet, Th*M*α: synthetic ThO_2, F*K*α: fluorite, S*K*α: barite. Strontium, Ba, Fe, Zr, U, P and Cl were sought but not found. The raw data were corrected using

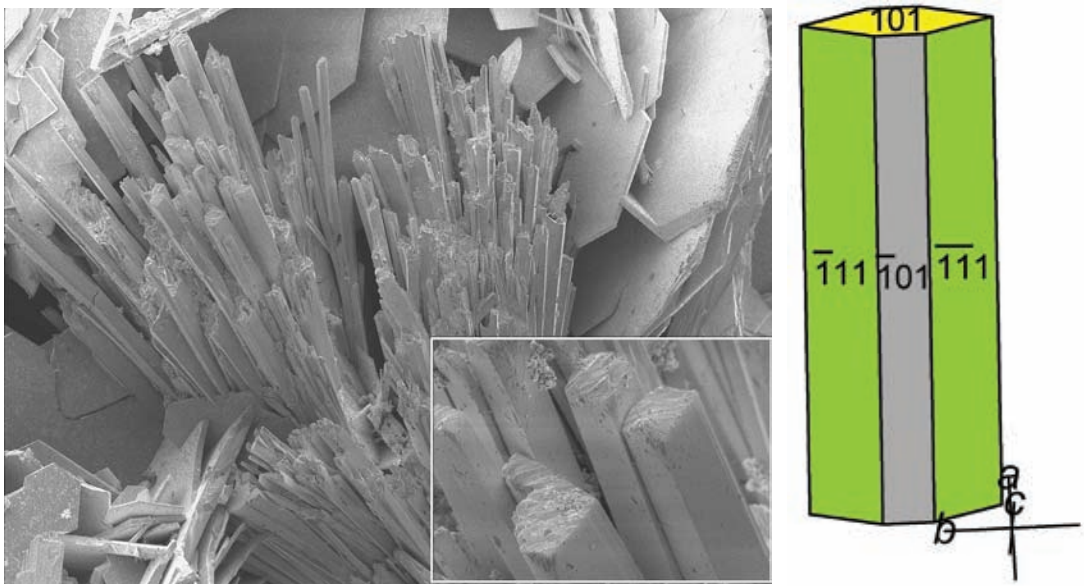

FIG. 1. Bussyite-(Ce): (a) SEM image of a spray of bussyite-(Ce) with hexagonal plates of catapleiite. Maximum dimension of image is 1.5 mm. Inset shows detail of crystal terminations. (b) Crystal morphology.

a PAP correction routine (Pouchou & Pichoir 1984) as part of the XMQANT package (pers. commun. C. Davidson, CSIRO).

Two distinct phases were analyzed (Fig. 2). The amount of H_2O in the hydrous phase (type material) was calculated from the structural formula, and its presence was verified by infrared analyses. The amount of BeO was measured with ToF–SIMS, as described below. In total, 26 analyses were performed on three separate samples for the low-Na (common) phase and three analyses were made on the high-Na (rare) phase. Empirical formulas based on these data and arranged in conjunction with the crystal-structure refinement are: $4\{(Ce_{0.823}Nd_{0.373}Y_{0.242}Th_{0.173}Pr_{0.103}Sm_{0.079}Gd_{0.078}Eu_{0.008})_{\Sigma 1.879}(Ca_{0.775}La_{0.225})_{\Sigma 1}[Na_{3.000}(H_2O)_{2.500}Ca_{0.544}K_{0.015}]_{\Sigma 6.055}(Mn_{0.485}Na_{0.402}Mg_{0.012})_{\Sigma 0.899}(Si_{8.897}Be_{4.605}Al_{0.222})_{\Sigma 13.724}O_{30}[F_{2.67}(OH)_{1.33}]_{\Sigma 4}\}$ for the low-Na phase and $4\{(Ce_{1.047}Nd_{0.466}La_{0.323}Y_{0.306}Pr_{0.131}Sm_{0.102}Gd_{0.084}Eu_{0.009}Th_{0.042})_{\Sigma 2.510}(Na_{6.645}Ca_{0.701})_{\Sigma 7.346}(Si_{9.521}Be_{4.772})_{\Sigma 14.293}(O_{29.251}F_{4.749})_{\Sigma 34}\}$ for the anhydrous high-Na phase.

Time of flight – secondary-ion mass spectrometry

The ToF–SIMS measurements for Be were acquired at Surface Science Western using an ION–TOF (GmbH), ToF–SIMS IV. The upgraded instrument is equipped with a state-of-the-art Bismuth Liquid Metal Ion Source (LMIG). The sample was mounted on a stainless steel sample stage with metal clips and then introduced into the ToF–SIMS instrument for analysis under ultra-high-vacuum conditions. The primary beam was pulsed 25 keV Bi^+ with a ~1.5 μm spot size and a target current of ~0.6 pA. The ToF–SIMS data were collected by rastering the Bi^+ primary beam over an area approximately 180 μm^2. The interaction of the primary ion beam on the sample surface induces the emission of positive and negative secondary ions (as well as neutral species). These secondary ions are extracted from the sample surface and mass-separated *via* the ToF analyzer. The mass resolution for this work was ~10,000 above 200 amu, and the mass range was 0–1000 amu. Owing to the insulating nature of the samples, a pulsed-electron flood gun was employed for charge neutralization. The

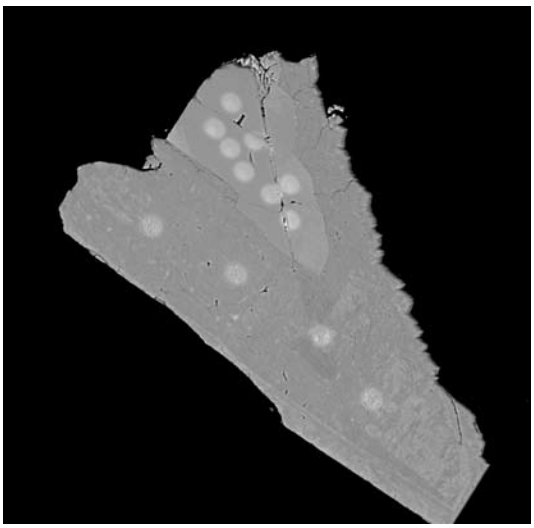

FIG. 2. Back-scattered electron image of a fragment of a bussyite-(Ce) crystal. Lighter grey patch is the anhydrous, high-Na portion, whereas the darker grey area is the more common hydrous, Na-poor phase. White circles mark the locations of electron-microprobe analyses. Maximum dimension of image is 350 μm.

TABLE 1. COMPOSITION OF BUSSYITE-(Ce) AND THE ASSOCIATED HIGH-Na PHASE

	Sample averages			Statistics for all analytical data				High-Na phase
n	06-11 6	06-02 8	UK-118 9	Average	Max	Min	Std. Dev	06-02 3
Na_2O wt.%	7.92	7.24	7.72	7.63	9.40	6.62	0.69	14.37
K_2O	0.11	0.03	0.02	0.05	0.13	0.00	0.05	0.00
BeO†	8.33	8.33	8.33	8.33				8.33
CaO	5.06	5.62	5.36	5.35	5.95	4.17	0.41	2.74
MgO	0.04	0.05	0.01	0.03	0.11	0.00	0.04	0.00
MnO	2.44	2.56	2.47	2.49	3.00	1.71	0.40	0.00
Al_2O_3	0.64	1.03	0.79	0.82	1.54	0.39	0.26	0.00
Y_2O_3	1.72	2.19	2.02	1.97	2.68	1.51	0.33	2.41
La_2O_3	2.68	2.60	2.66	2.65	3.11	2.16	0.25	3.67
Ce_2O_3	10.27	9.15	9.89	9.77	11.22	8.15	0.77	12.00
Pr_2O_3	1.15	1.27	1.27	1.23	1.49	0.74	0.17	1.51
Nd_2O_3	4.64	4.37	4.60	4.54	5.13	3.91	0.33	5.48
Sm_2O_3	1.06	0.94	0.97	0.99	1.25	0.68	0.16	1.24
Eu_2O_3	0.13	0.09	0.09	0.10	0.25	0.00	0.09	0.11
Gd_2O_3	0.94	1.10	1.04	1.03	1.23	0.81	0.12	1.06
SiO_2	38.74	38.53	38.72	38.66	39.94	37.66	0.51	39.93
ThO_2	2.86	3.73	3.33	3.31	4.59	2.12	0.63	0.77
F	4.11	3.47	3.44	3.67	6.39	2.54	0.83	6.30
S	0.04	0.01	0.03	0.03	0.08	0.00	0.04	0.00
H_2O*	3.89	4.22	4.24	4.12	4.59	2.83	0.39	0.00
O=F	-1.73	-1.46	-1.45	-1.55	-1.07	-2.69	-0.35	-2.65
O=S	-0.02	-0.01	-0.01	-0.01	0.00	-0.04	-0.02	0.00
Total	95.00	95.04	95.54	95.21				97.27
Na *apfu*	3.539	3.229	3.437	3.402	4.168	2.968	0.296	6.645
K	0.032	0.010	0.005	0.015	0.038	0.000	0.016	0.000
Be	4.616	4.605	4.596	4.605	4.661	4.515	0.037	4.772
Ca	1.252	1.386	1.320	1.319	1.465	1.022	0.104	0.701
Mg	0.013	0.019	0.004	0.012	0.039	0.000	0.013	0.000
Mn^{2+}	0.476	0.499	0.480	0.485	0.582	0.333	0.079	0.000
Al	0.173	0.280	0.214	0.222	0.420	0.104	0.072	0.000
Y	0.211	0.268	0.246	0.242	0.332	0.186	0.040	0.306
La	0.228	0.220	0.225	0.225	0.265	0.186	0.020	0.323
Ce	0.867	0.771	0.831	0.823	0.940	0.690	0.063	1.047
Pr	0.097	0.106	0.106	0.103	0.124	0.063	0.014	0.131
Nd	0.382	0.359	0.377	0.373	0.413	0.320	0.026	0.466
Sm	0.085	0.074	0.077	0.079	0.099	0.054	0.013	0.102
Eu	0.011	0.007	0.007	0.008	0.020	0.000	0.007	0.009
Gd	0.072	0.084	0.080	0.078	0.093	0.062	0.009	0.084
Si	8.935	8.865	8.892	8.897	9.033	8.772	0.066	9.521
Th	0.150	0.195	0.174	0.173	0.243	0.110	0.034	0.042
F	2.996	2.520	2.498	2.672	4.640	1.871	0.599	4.749
S	0.017	0.004	0.011	0.011	0.036	0.000	0.016	0.000
H	5.987	6.476	6.491	6.318	7.129	4.327	0.605	0.000
O	30.987	31.476	31.491	31.318	32.129	29.327	0.605	29.251
Σcations	21.137	20.975	21.073	21.061				24.150

The number of atoms per formula unit (*apfu*) is based on 34 anions. † The amount of Be is based on TOF–SIMS data on 06-02. The other analytical data were acquired by electron-microprobe analysis; *n*: number of analyses made. * H_2O calculated assuming 4(F,OH) plus 2.5 structural H_2O for low-Na phase.

concentration of Be in bussyite-(Ce) was determined through comparison of intensities of $^{9}Be^{+}$ and $^{28}Si^{+}$ secondary ions collected from a leucophanite reference standard. The Be concentration in bussyite-(Ce) was calculated according to the relation: wt.% $Be_{bussyite}$ = (wt.% $Be_{leucophanite}$) × (wt.% $Si_{bussyite}/Si_{leucophanite}$) ($^{9}Be^{+}$ / $^{28}Si^{+}_{bussyite}$)/($^{9}Be^{+}$ / $^{28}Si^{+}_{leucophanite}$).

Infrared analysis

The infrared spectrum (Fig. 3) of bussyite-(Ce) was obtained using a Bomen Michelson MB–120 Fourier-transform infrared spectrometer with a diamond-anvil cell as a microsampling device. The frequencies are not well resolved. The large, broad (3600 to 2700 cm^{-1}) peak centered in the 3421 cm^{-1} region is the O–H or H–O–H stretching frequency, indicating the presence of an $[OH]^{-}$ or an $[H_2O]$ group. The H–O–H bend region (1690–1580 cm^{-1}) and centered at 1645 cm^{-1} is a clear indication of H_2O being present in the structure. Comparing the remaining part of the spectrum to spectra given in Farmer (1974), the following frequency-regions are assigned modes: the large, broad peak centered at 993 cm^{-1} is the $[SiO_4]$ and $[BeO_4]$ stretching mode; the moderate-intensity sharp peak centered at 705 cm^{-1} is $[SiO_4]$ and $[BeO_4]$ bending mode, and the moderate-intensity sharp peak centered at 503 cm^{-1} is another $[SiO_4]$ bending mode.

Digital versions of the spectra are available from the Depository of Unpublished Data on the MAC website [document: Bussyite-(Ce) CM47_193].

X-Ray Crystallography and Crystal-Structure Determination

The X-ray powder-diffraction data (Table 2) were collected with a Bruker AXS Discover 8 microdiffractometer using Hi-Star 2-D area detector operated with a GADDS system, Cu$K\alpha_1$ radiation at 40 kV and 40 mA, with a sample-to-detector distance of 12 cm. The instrument was calibrated with synthetic corundum (Powder Diffraction File 10–0173) using an as-yet-unpublished statistical calibration elaborated at the Canadian Museum of Nature that allows for more accurate sample-to-detector distance and detector-center coordinates, thus increasing experimental accuracy. Cell refinement of the measured powder pattern was obtained by indexing the diffraction maxima using intensities from a powder pattern calculated using atom coordinates determined in the crystal-structure analysis.

To obtain a single crystal of bussyite-(Ce), free of twinned individuals, a cleavage fragment was trimmed.

TABLE 2. BUSSYITE-(Ce): X-RAY POWDER-DIFFRACTION DATA[§]

I obs	*I* calc *	*d* obs	*d* calc **	*h k l*	*I* obs	*I* calc *	*d* obs	*d* calc **	*h k l*
100	100	8.120	8.108	$\bar{1}$ 1 1	10	6	2.232	2.232	0 2 7
26	16	6.959	6.958	0 2 0	2	3	2.151	2.157	0 4 6
6	5	6.296	6.303	$\bar{1}$ 1 2	2	3	2.135	2.134	$\bar{3}$ 5 3
5	5	5.327	5.318	0 2 2	3	3	2.103	2.103	$\bar{2}$ 6 2
9	8	4.523	4.523	1 1 3		8		2.081	$\bar{5}$ 3 1
10	5	4.484	4.454	$\bar{2}$ 2 0	7	2	2.076	2.077	$\bar{2}$ 4 6
13	14	4.210	4.206	$\bar{1}$ 3 1	7	3	2.068	2.068	1 5 5
7	4	4.118	4.124	0 0 4		2		2.064	2 6 2
7	8	4.066	4.054	$\bar{2}$ 2 2	8	8	2.028	2.027	$\bar{4}$ 4 4
6	8	3.781	3.796	2 2 2	4	4	2.009	2.009	$\bar{2}$ 0 8
4	4	3.727	3.727	$\bar{3}$ 1 0	3	3	1.9441	1.9496	$\bar{1}$ 7 1
	20		3.558	3 1 1		2		1.9418	1 7 1
39	19	3.543	3.548	0 2 4	11	5	1.9253	1.9322	6 0 0
21	20	3.454	3.455	$\bar{1}$ 3 3		10		1.9207	$\bar{3}$ 3 7
5	5	3.323	3.330	1 3 3		3		1.9083	3 1 7
11	14	3.236	3.234	$\bar{3}$ 1 3	4	1	1.9015	1.9003	4 0 6
19	17	3.176	3.176	$\bar{1}$ 1 5	2	3	1.8785	1.8798	2 6 4
	8		3.152	$\bar{2}$ 2 4	9	10	1.8343	1.8357	1 7 3
6	5	3.019	3.018	1 1 5		2		1.8177	2 2 8
24	22	2.959	2.963	$\bar{3}$ 3 1	3	3	1.8128	1.8139	3 5 5
	7		2.951	3 1 3	11	12	1.7728	1.7792	3 3 7
48	34	2.863	2.883	3 3 1		2		1.7728	0 6 6
	44		2.853	$\bar{2}$ 4 2	8	7	1.7402	1.7395	$\bar{2}$ 4 8
23	23	2.749	2.749	0 0 6		3		1.7395	0 8 0
33	22	2.668	2.668	$\bar{1}$ 3 5	10	8	1.6990	1.6984	$\bar{4}$ 6 4
	7		2.659	0 4 4		6		1.6976	$\bar{1}$ 7 5
	18		2.651	4 0 2		5		1.6879	5 3 5
3	3	2.574	2.572	1 3 5	9	8	1.6848	1.6849	6 0 4
4	6	2.493	2.494	$\bar{4}$ 0 4		2		1.6846	$\bar{6}$ 4 2
2	3	2.390	2.391	2 0 6	9	3	1.6621	1.6627	$\bar{6}$ 0 6
12	15	2.355	2.359	2 4 4	3	3	1.6326	1.6266	6 4 2
	3		2.357	3 1 5	5	3	1.6221	1.6216	$\bar{5}$ 5 5
11	5	2.320	2.319	0 6 0		3		1.6047	4 0 8
7	6	2.290	2.288	$\bar{1}$ 5 4	3	2	1.6021	1.6028	0 8 4
9	8	2.257	2.258	3 5 0					

* calculated based on results from crystal-structure determination.
** calculated from XRPD unit-cell refinement with *a* 11.654(3), *b* 13.916(3), *c* 16.583(4) Å, β 95.86(2)°, *V* 2675.4(8) Å^3. § Cu$K\alpha_1$ radiation.

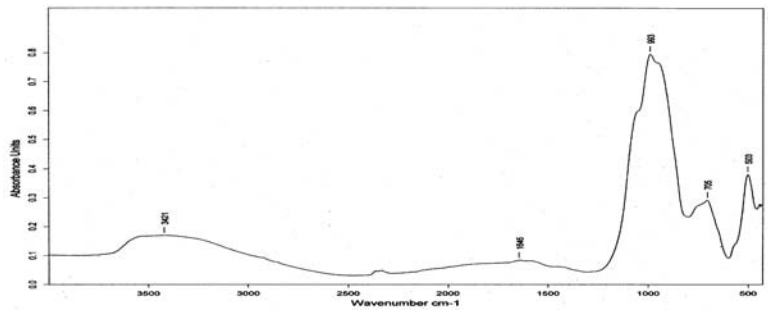

FIG. 3. Infrared absorption spectra for bussyite-(Ce).

Data on two such crystals were collected. To determine the structure, we used the X-ray-diffraction intensity data for the larger of the two crystals, measuring 40 × 60 × 200 μm. Data for the smaller crystal were not as good as for the larger, even with doubling of the collection time. Intensity data were collected on a fully automated Bruker *P*4 four-circle diffractometer operated at 50 kV, 40 mA, with graphite-monochromated Mo*K*α radiation and a 4K APEX CCD detector located 6 cm from the crystal. Integrated intensities were collected up to 2θ = 55°, using 60 s frame counts and a frame width of 0.2°. The intensity of spots beyond 40°2θ is very diffuse; this became the maximum 2θ used in the structure refinement. Data pertinent to the intensity-data collection are given in Table 3. The unit-cell parameters for the single crystal were refined using 3538 indexed reflections.

Reduction of the intensity data, structure determination and structure refinement were done with the SHELXTL (Sheldrick 1990) package of computer programs. Data reduction included corrections for background, scaling and Lorentz-polarization factors. An empirical absorption correction (SADABS, Sheldrick 1998) was applied. The merging $R_{(int)}$ for the dataset (8631 reflections) decreased from 0.049 before the absorption correction to 0.037 after the absorption correction. Assigning phases to a set of normalized structure-factors gave a mean $|E^2 - 1|$ value of 0.995, suggesting the centrosymmetric space-group, *C*2/*c*. The phase-normalized structure-factors were used to construct an *E*-map on which were located positions for 20 atoms. These initial sites were refined, and new sites added. Eventually, the correct scattering curves could be assigned to each site. In the refinement process, it became evident that two sites, *Na*4 and *Si*5, were best refined as split sites. Both of these have a special function within the crystal structure, as is discussed below. In an attempt to resolve these split sites, the structure was also solved in noncentrosymmetric space-group *Cc*. The data did not refine nearly as well in this space group as in the centrosymmetric one, *C*2/*c*, and the problem of split sites was not resolved. In the last stages of refinement, there were electron residuals of +1.4 and –2.0 e$^-$/Å^3. In the final least-squares refinement, all atom positions were refined with anisotropic displacement-factors. The weighting scheme is inversely proportional to $\sigma^2(F)$. The addition of an isotropic extinction-correction did not improve the refinement. The data did not yield a high-quality refinement, with respect to standard deviations in the bond lengths, but both crystals gave the exact same model and similar residuals, *R*, of 4.0%. The final positional and anisotropic displacement-parameters are given in Table 4, and selected bond-lengths and angles, in Table 5. Tables listing the observed and calculated structure-factors may be obtained from the Depository of Unpublished Data on the MAC website [document: Bussyite-(Ce) CM47_193].

TABLE 3. BUSSYITE-(Ce): DATA COLLECTION AND STRUCTURE-REFINEMENT INFORMATION

Space group	*C*2/*c*	Measured reflections	4564
a (Å)	11.6445(6)	Unique reflections	1252
b (Å)	13.9212(8)	Observed reflections [> 4σ(*F*)]	1134
c (Å)	16.5909(9)	*R*(int) (%)	2.8
β (°)	96.127(1)	Goodness of fit on F^2	1.16
V (Å^3)	2674.1(4)	*R* index (%) for all data	4.6
μ (mm^{-1})	5.86	*R* index (%) for observed data	4.0

Ideal unit-cell contents: $4[(Ce,Ca)_3(Na,H_2O)_6Mn(Si,Be)_{14}(O,OH)_{36}(F,OH)_4]$

DESCRIPTION OF THE STRUCTURE

In the structure of bussyite-(Ce), there are two sites containing the rare-earth elements (REE) and Ca, both with 8-fold coordination. There is partitioning in these two sites, with one site having a larger scattering factor, a smaller, average bond-length and a higher bond-valence. To satisfy these conditions, site assignments were as follows: the *Ce* site contains the smaller REEs and Th, $(Ce_{0.823}Nd_{0.373}Y_{0.242}Th_{0.173}Pr_{0.103}Sm_{0.079}Gd_{0.078}Eu_{0.008})_{\Sigma 1.879}$; this gives 111.6 e^- compared with the structure-refined site occupancy of 109.0 e^-. Arguably Ce is only slightly smaller than La, but the other REEs and Th in this site are appreciably smaller that La or Ca. The *Ca* site contains the larger Ca and La: $(Ca_{0.775}La_{0.225})_{\Sigma 1}$; this gives 28.3 e^-, which matches the structure-refined site occupancy, 28.7 e^-. The *Na* sites are quite varied in types of polyhedra. The *Na*1 and *Na*2 sites are both bonded to 6 O and 2 F atoms. These polyhedra are triangular dodecahedra. The *Na*3 site is seven-coordinated with 6 O and 1 F. The polyhedron may be described as a pentagonal bipyramid. The *Na*3 site has adjacent voids that could facilitate the incorporation of an H_2O group, as described later in the text. The *Na*4 site is split, creating a rather large space within the layer. This large-volume site is the most probable location for a H_2O group. The four *Na* sites ideally hold six cations. In this structure refinement, the four sites are assigned all of the Na, the Ca remaining from the *Ca*,*La* site and H_2O groups: $[Na_{3.000}(H_2O)_{\Sigma 2.5}Ca_{0.544}K_{0.015}]_{\Sigma 6.059}$; this gives 69.2 e^-, compared with the structure-refined occupancy of 66.7 e^-. The 6-fold coordination site, which probably held Na in the anhydrous phase, is a distorted octahedron. It contains the remaining Na and the Mn, which was introduced during hydration: $(Mn_{0.485}Na_{0.402}Mg_{0.012})_{\Sigma 0.899}$; this gives 16.7 e^- compared with the structure-refined occupancy of 15.8 e^-.

The tetrahedrally coordinated sites are varied, with three regular $[SiO_4]$ tetrahedra at the *Si*1, *Si*3 and *Si*4 sites and two regular $[BeO_3F]$ tetrahedra at the *Be*6 and *Be*7 sites, with only very minor substitution of Si for Be. The *SiBe*2 site is approximately half-populated by Si and half by Be. In order for this to be possible, there must be OH ligands. From Table 4, it is evident from the bond-valence sums that this is the case in the *O*5, *O*8 and *O*9 sites. The *Si*5 site is split into two

sites 1.21 Å apart. Using the Si-scattering curve, the site-occupancy factor (sof) was found to be 0.65(1) at the *Si*5 site and 0.28(1) at the *Si*5a site. To adjust this to a site occupancy of 1, the *Si*5a site was allowed to refine with Be as well. There is little indication of Be (about 20%) at site *Si*5a and zero at site *Si*5. The bond lengths (Table 5) for both *Si*5 sites are long for normal Si–O bonds. For this reason, the small amount of Al was assigned to this site, as Al–O bonds are longer than Si–O bonds. Figure 4 shows the split *T*5 site with tetrahedra pointing in opposite directions. This polarity shift has implications for the sheet structure discussed in the following section. Of interest is that in the second crystal studied, this site was split in a similar fashion with a 0.75:0.25 proportion of scattering and without

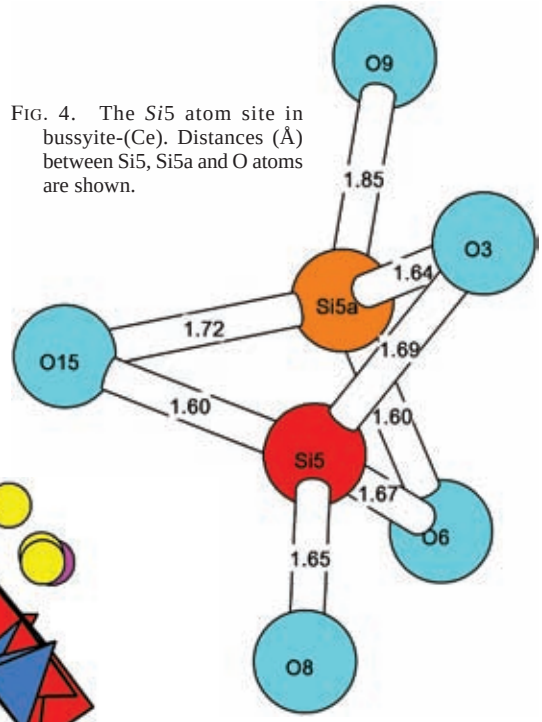

FIG. 4. The *Si*5 atom site in bussyite-(Ce). Distances (Å) between Si5, Si5a and O atoms are shown.

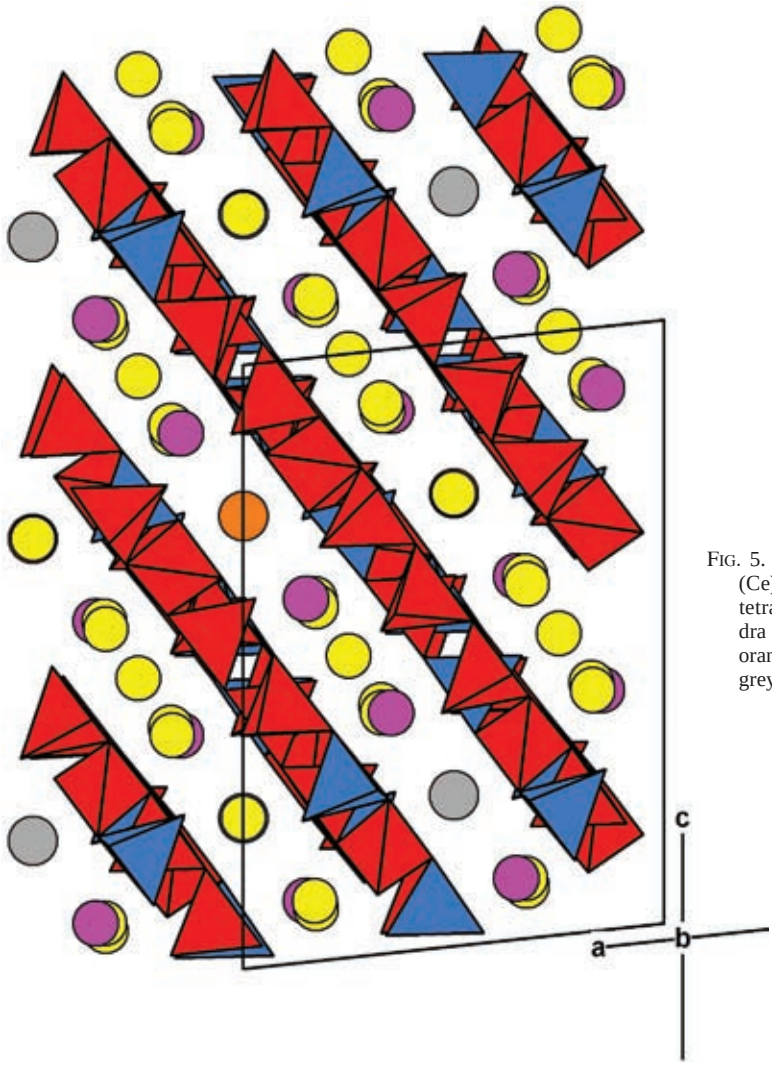

FIG. 5. The layered structure of bussyite-(Ce) projected along [010]. The [SiO_4] tetrahedra are red, the [BeO_4] tetrahedra blue, Ce atoms in red, Ca atoms in orange, Na atoms in yellow, and Mn in grey.

indication of any Be in either portion. The total Be as determined by crystal-structure analysis is 5.05 *apfu*. This is higher than that determined by SIMS ToF, 4.60 *apfu*, but we believe it to be more accurate. The 5.05 atoms of Be would increase the wt.% BeO to 9.80, which would bring the total to 96.68 wt.%.

Bussyite-(Ce) has a distinctly layered structure (Fig. 5) consisting of two slabs of polyhedra; (1) a sheet of Si–Be tetrahedra and (2) a large slab of Ce–Na–Mn–O polyhedra. Slabs are cross-linked through shared O atoms, but only weakly so, as indicated by the perfect ($10\bar{1}$) cleavage. The sheet of tetrahedra will have two different topologies depending on the site occupancy of *Si*5. If the *Si*5 site is fully occupied, then the topology is that in Figure 6a. Chains of Si and Be tetrahedra are cross-linked by the *Si*4 site tetrahedra. The chains are a loop-branched zehner single chains (Liebau 1985). If the *Si*5a site is fully occupied, then the topology is that in Figure 6b. The layer of tetrahedra is still a sheet, but it has a rather large "S"-shaped void in it. The second slab of polyhedra consists of the larger cations Ce, Na, Ca and Mn. The polyhedra of this layer (Fig. 7) are in two distinct chains; the higher bond-valence cations Ce, Ca and Mn form one chain of polyhedra that is cross-linked to the chain of Na polyhedra. It is this striking topological feature that lends itself to hydration within this layer. The chain of Na polyhedra may be replaced in part by H_2O groups or $(OH)^-$ ions, particularly in the split (disordered) *Na*4 site and the *Na*3 site with adjacent voids (Fig. 7). Looking closely at the crystal termination (Fig. 1a), the roughness would be a morphological expression of the layered crystal structure, and hydrothermal alteration of these crystals would enhance this uneven texture.

TABLE 4. BUSSYITE-(Ce): ATOMIC COORDINATES, ANISOTROPIC DISPLACEMENT FACTORS (Å^2) AND BOND-VALENCE SUMS (*vu*)

Atom	*x*	*y*	*z*	sof**	U_{11}	U_{22}	U_{33}	U_{23}	U_{13}	U_{12}	U_{eq}	BVS
RE1 (Ce)	0.14869(1)	0.25501(1)	0.39821(3)	0.9404(1)	0.0168(1)	0.0140(1)	0.0140(1)	-0.0005(1)	-0.0011(1)	-0.0005(1)	0.01515(3)	2.45
Ca	0	0.45863(2)	¼	0.3820(2)	0.0199(2)	0.0228(2)	0.0186(2)	0	0.0013(1)	0	0.0205(1)	2.14
La	0	0.45863(2)	¼	0.1180(2)	0.0199(2)	0.0228(2)	0.0186(2)	0	0.0013(1)	0	0.0205(1)	2.14
Na1	0	0.7389(1)	¼	0.573(1)	0.0535(5)	0.0313(5)	0.0316(5)	0	0.0174(4)	0	0.0378(2)	1.09
Na2	0.1686(1)	0.5435(1)	0.4004(1)	1	0.0170(4)	0.0671(5)	0.0169(3)	-0.0118(4)	-0.0007(3)	-0.0047(4)	0.0339(2)	1.16
Na3	0.1725(1)	0.9802(1)	0.4124(1)	0.950(2)	0.0361(4)	0.0530(4)	0.0476(4)	0.0290(4)	0.0081(4)	0.0026(4)	0.0453(2)	1.11
Na4	0.1874(2)	0.2469(1)	-0.0382(1)	0.507(2)	0.076(1)	0.030(1)	0.068(1)	0.000(1)	0.025(1)	-0.006(1)	0.0566(5)	1.20
Mn	0	0.07534(3)	¼	0.3178(4)	0.0259(4)	0.0477(3)	0.0280(3)	0	-0.0016(3)	0	0.0342(2)	2.25
Si1	0.20532(4)	0.90024(3)	0.23466(3)	1	0.0315(3)	0.0261(3)	0.0243(3)	-0.0029(2)	-0.0007(4)	0.0003(4)	0.0276(1)	3.88
Si2	0.0815(1)	1.1056(1)	0.0615(1)	0.463(1)	0.0164(4)	0.0140(4)	0.0156(4)	0.0025(4)	-0.0007(4)	0.0007(4)	0.0154(2)	3.02
Be2	0.0815(2)	1.1056(2)	0.0615(1)	0.537(1)	0.0164(1)	0.0140(4)	0.0156(4)	0.0025(4)	-0.0007(4)	0.0007(4)	0.0153(2)	3.02
Si3	0.08092(4)	0.60954(3)	0.08162(3)	1	0.0291(3)	0.0292(3)	0.0247(3)	0.0024(3)	-0.0020(3)	-0.0063(3)	0.0280(2)	3.91
Si4	0.16350(4)	0.25345(3)	0.17442(3)	1	0.0251(3)	0.0228(3)	0.0213(3)	-0.0015(2)	-0.0033(2)	-0.0014(2)	0.0235(2)	3.91
Si5	0.0919(1)	0.8886(1)	0.0736(1)	0.640(3)	0.0236(4)	0.0036(3)	0.0153(4)	-0.0001(3)	0.0011(3)	0.0012(3)	0.0142(2)	3.68
Si5a	0.0521(2)	0.8108(2)	0.0873(1)	0.209(4)	0.027(1)	0.036(1)	0.020(1)	-0.007(1)	-0.003(1)	0.005(1)	0.026(1)	1.86
Be5a	0.0521(4)	0.8108(2)	0.0873(1)	0.151(4)	0.027(1)	0.030(1)	0.020(1)	-0.007(1)	-0.003(1)	0.005(1)	0.026(1)	1.86
Be6*	0.2523(2)	0.6025(1)	0.2191(1)	0.957(1)	0.010(1)	0.007(1)	0.016(1)	-0.000(1)	0.009(1)	0.003(1)	0.010(1)	1.89
Be7*	0.0479(2)	0.4041(1)	0.0780(1)	0.961(1)	0.011(1)	0.012(1)	0.030(1)	-0.004(1)	0.005(1)	0.000(1)	0.018(1)	1.89
O1	0.3177(1)	0.8954(1)	0.1852(1)	1	0.020(1)	0.016(1)	0.020(1)	-0.002(1)	0.009(1)	0.004(1)	0.0179(3)	1.80
O2	0.1794(1)	1.0027(1)	0.2720(1)	1	0.023(1)	0.016(1)	0.023(1)	-0.003(1)	0.011(1)	0.005(1)	0.0200(4)	2.22
O3	0.0892(1)	0.8687(1)	0.1721(1)	1	0.017(1)	0.032(1)	0.021(1)	-0.006(1)	-0.005(1)	-0.006(1)	0.0237(4)	1.97
O4	0.2810(1)	0.3196(1)	0.1906(1)	1	0.029(1)	0.020(1)	0.018(1)	-0.008(1)	-0.006(1)	-0.012(2)	0.0230(4)	1.98
O5	-0.0272(1)	1.1084(1)	0.1110(1)	1	0.014(1)	0.017(1)	0.013(1)	-0.001(1)	0.003(1)	-0.004(1)	0.0146(3)	1.67
O6	0.0448(1)	1.1292(1)	-0.0358(1)	1	0.023(1)	0.033(1)	0.017(1)	-0.000(1)	-0.002(1)	0.011(1)	0.0242(4)	2.14
O7	0.1806(1)	0.1820(1)	0.0987()	1	0.026(1)	0.023(1)	0.023(1)	-0.006(1)	0.004(1)	-0.001(1)	0.0238(4)	2.12
O8	0.1414(2)	0.9996(1)	0.0602(1)	1	0.047(1)	0.027(1)	0.036(1)	-0.003(1)	0.014(1)	0.006(1)	0.0364(4)	1.71
O9	-0.0053(1)	0.6925(1)	0.1138(1)	1	0.059(1)	0.033(1)	0.034(1)	-0.002(1)	0.006(1)	0.019(1)	0.0420(4)	1.58
O10	0.2131(1)	0.6250(1)	0.1206(1)	1	0.011(1)	0.022(1)	0.011(1)	0.005(1)	-0.004(1)	-0.007(1)	0.0153(3)	1.94
O11	0.0713(1)	0.6199(1)	-0.0168(1)	1	0.031(1)	0.034(1)	0.005(1)	0.005(1)	-0.004(1)	-0.012(1)	0.0240(4)	1.77
O12	0.0320(1)	0.5091(1)	0.1132(1)	1	0.027(1)	0.013(1)	0.024(1)	-0.000(1)	-0.000(1)	-0.005(1)	0.0214(4)	2.08
O13	0.0504(1)	0.3220(1)	0.1512(1)	1	0.015(1)	0.020(1)	0.020(1)	0.000(1)	-0.000(1)	-0.000(1)	0.0186(3)	1.88
O14	0.1547(1)	0.1909(1)	0.2557(1)	1	0.018(1)	0.013(1)	0.007(1)	0.003(1)	-0.002(1)	-0.002(1)	0.0130(3)	2.09
O15	0.3278(1)	0.3109(1)	0.4643(1)	1	0.018(1)	0.022(1)	0.014(1)	0.007(1)	-0.008(1)	-0.002(1)	0.0185(3)	1.81
F16	0.1390(1)	0.6014(1)	0.2656(1)	1	0.037(1)	0.029(1)	0.046(1)	-0.001(1)	0.008(1)	-0.002(1)	0.0372(3)	0.90
F17	0.1620(1)	0.3990(1)	0.0303(1)	1	0.040(1)	0.055(1)	0.042(1)	0.008(1)	0.004(1)	0.002(1)	0.0460(4)	0.87

Bond-valence sum (BVS) using constants of Brese & O'Keeffe (1991). * Atom ratios: Be6 : Si6 = 0.94 : 0.06; Be7 : Si7 = 0.96 : 0.04. ** sof: site-occupancy factor. Scattering curve is that used in atom name.

TABLE 5. BUSSYITE-(Ce): SELECTED BOND-LENGTHS (Å)

RE1-O15	2.381(1)	Ca-O1 × 2	2.439(1)	Na1-O9 × 2	2.344(1)	Na2-F17	2.308(1)
RE1-O15*	2.447(1)	Ca-O12 × 2	2.442(1)	Na1-F16 × 2	2.502(1)	Na2-O8	2.321(1)
RE1-O1	2.451(1)	Ca-F16 × 2	2.558(1)	Na1-O3 × 2	2.510(1)	Na2-F16	2.368(1)
RE1-O11	2.463(1)	Ca-O13 × 2	2.618(1)	Na1-O4 × 2	2.863(1)	Na2-O12	2.371(1)
RE1-O10	2.471(1)	<Ca-O,F>	<2.514>	<Na1-O,F>	<2.555>	Na2-O1	2.518(1)
RE1-O5	2.479(1)					Na2-O7	2.607(1)
RE1-O14	2.535(1)					Na2-O9	2.806(1)
RE1-O13	2.552(1)					Na2-O11	2.946(1)
<RE1-O>	<2.472>					<Na2-O,F>	<2.531>
Na3-F17	2.347(1)	Na4-Na4	1.828(3)	Mn-O2 × 2	2.315(1)		
Na3-O6	2.355(1)	Na4-O7	2.163(2)	Mn-O5 × 2	2.340(1)		
Na3-O2	2.360(1)	Na4-O6	2.336(2)	Mn-O14 × 2	2.410(1)		
Na3-O5	2.461(1)	Na4-F17	2.436(2)	<Mn-O>	<2.355>		
Na3-O10	2.509(1)	Na4-O7*	2.454(2)				
Na3-O8	2.532(1)	Na4-O9	2.493(2)				
Na3-O4	2.901(1)	Na4-F17*	2.677(2)				
<Na3-O,F>	<2.495>	Na4-O4	2.754(2)				
		<Na4-O,F>	<2.473>				
Si1-O2	1.597(1)	Be,Si2-O5	1.580(1)	Si3-O10	1.618(1)	Si4-O14	1.618(1)
Si1-O1	1.618(1)	Be,Si2-O8	1.635(1)	Si3-O12	1.620(1)	Si4-O7	1.631(1)
Si1-O3	1.673(1)	Be,Si2-O6	1.658(1)	Si3-O11	1.631(1)	Si4-O13	1.638(1)
Si1-O4	1.667(1)	Be,Si2-O7	1.641(1)	Si3-O9	1.657(1)	Si4-O4	1.648(1)
<Si1-O>	<1.639>	<Be,Si2-O>	<1.628>	<Si3-O>	<1.632>	<Si4-O>	<1.634>
Si5-Si5a	1.210(2)	Si5a-Si5	1.210(2)	Be6-F16	1.597(2)	Be7-F17	1.592(2)
Si5-O15	1.602(1)	Si5a-O6	1.580(2)	Be6-O2	1.600(2)	Be7-O12	1.619(2)
Si5-O3	1.661(1)	Si5a-O3	1.639(2)	Be6-O14	1.663(2)	Be7-O13	1.666(2)
Si5-O6	1.667(1)	Si5a-O15	1.716(2)	Be6-O10	1.679(2)	Be7-O11	1.665(2)
Si5-O8	1.672(1)	Si5a-O9	1.848(2)	<Be6-O,F>	<1.635>	<Be7-O,F>	<1.636>
<Si5-O>	<1.651>	<Si5a-O>	<1.696>				

* A symmetry-related atom.

The role of hydrogen in bussyite-(Ce)

The new mineral species bussyite-(Ce) is an intimate association of two closely related phases; the rare anhydrous bussyite patches in a primarily hydrous bussyite (Fig. 2). The crystal structure-analysis was done on a composite crystal. As there is no splitting of the diffraction spots, it can be assumed the cell volumes of the two phases are essentially identical. There are several differences in the chemical composition of the two phases; the hydrated phase has less Na, and F and more Th, Al, Mn, and Ca than its anhydrous counterpart. We cannot say anything about differences in Be as the analysis was of a whole crystal, consisting of both phases (Table 1, sample 06–02). Hydration of the precursor anhydrous phase could readily proceed along the chains of Na polyhedra described above. Sodium, having a low bond-valence, could easily be replaced by H_2O, which would be H-bonded to surrounding anions and weakly bonded to remaining Na, Ce, Mn and Ca cations. The Na sites that easily accommodate H_2O groups are *Na*3 and *Na*4. Hydroxyl anions are also involved in the hydration of bussyite. From the results of chemical analyses of both phases, there is direct evidence of OH substitution for F. In addition, the bond-valence sums for O sites *O*5, *O*8 and *O*9 all indicate some substitution of OH for O. Each of these are bonded to a mixed Si,Be site, allowing for this type of substitution. To date, we have not found a crystal of the parent, anhydrous phase. If it is observed at all, it is only as small patches within hydrous bussyite-(Ce).

Related structures

In the structural hierarchy for beryllium minerals, given in an overview by Hawthorne & Huminicki (2002), 17 beryllium silicate layered structures are listed, of which ten have unique structures. The melilite-type structures were discussed by Grice & Hawthorne (2002). If we consider the sheet of tetrahedra as a two-dimensional net (Smith 1977, Hawthorne & Smith 1986), members of the melilite group have pentagonal nets that are 3- and 4-connected. Grice & Hawthorne (2002) pointed out that aminoffite does not belong to the melilite group, as had been previously considered, as it has a more complex layer of 4- and 6-connected nets (Fig. 8a). The topology of the layer of tetrahedra in bussyite-(Ce) is even more complicated than that in aminoffite. It is composed of 4-, 5, and 8-connected nets, with a topology formula of $(4.5.8)_2(5^2.8)(5^2.8^2)$ (Fig. 8b). This topology more closely resembles that of the layers of tetrahedra of semenovite-(Ce) and harstigite (Figs. 8c, d). The crystal structure of semenovite-(Ce) (Mazzi *et al.* 1979) has the topology

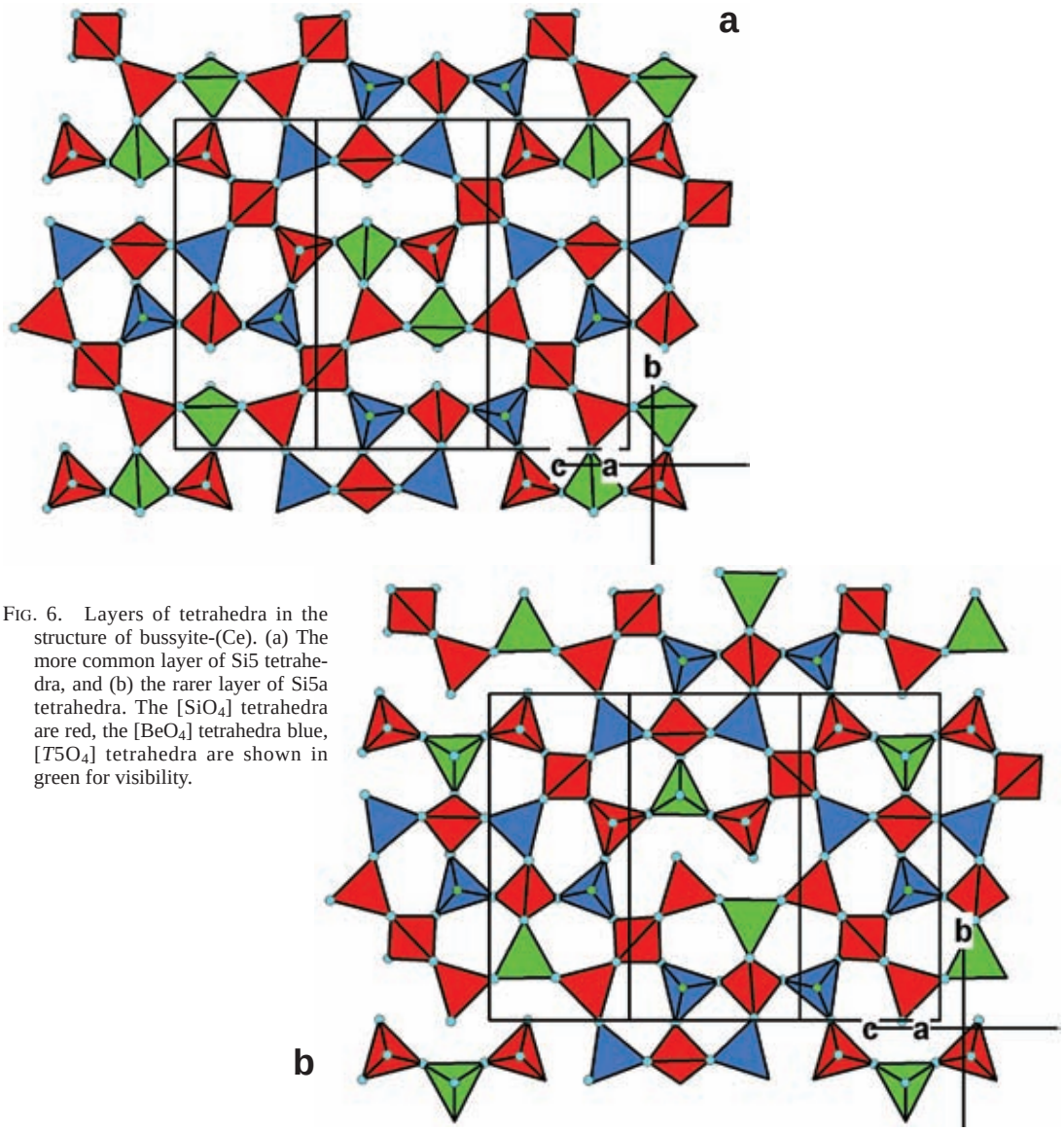

FIG. 6. Layers of tetrahedra in the structure of bussyite-(Ce). (a) The more common layer of Si5 tetrahedra, and (b) the rarer layer of Si5a tetrahedra. The [SiO_4] tetrahedra are red, the [BeO_4] tetrahedra blue, [$T5O_4$] tetrahedra are shown in green for visibility.

$(4.5^2)_2(4.5^2.8)(5^2.8)_2$, whereas the structure of harstigite (Hesse & Stümpel 1986) has the topology $(4.5^2)(4.5^2.8)(5^2.8)_2$. These two very similar topologies differ in their formula by a variation in the Si:Be ratio in the two structures. Ignoring the differentiation of [BeO_4] and [SiO_4] tetrahedra, the layers of tetrahedra in semenovite-(Ce) and harstigite are identical. Recognizing this fact, it is apparent that these two minerals are almost isostructural. If we expand the search for structural similarities to framework silicates, aluminosilicates and beryllium silicates, we find only two minerals and no synthetic phases that are built from 4-, 5- and 8-connected nets: montesommaite and yugawaralite. Both of these minerals have 2-dimensional nets that are comparable to that of semenovite-(Ce) and harstigite, with chains of 5-connected nets linked by bands of 4- and 8-connected nets. Only in epistilbite could the chains similar to those of bussyite-(Ce), 5-, 5-, 4-connected nets, be found, and these are cross-linked by 10-connected nets. It is evident that bussyite-(Ce) has a unique topology with no natural or synthetic counterparts with either 2- or 3-connect nets.

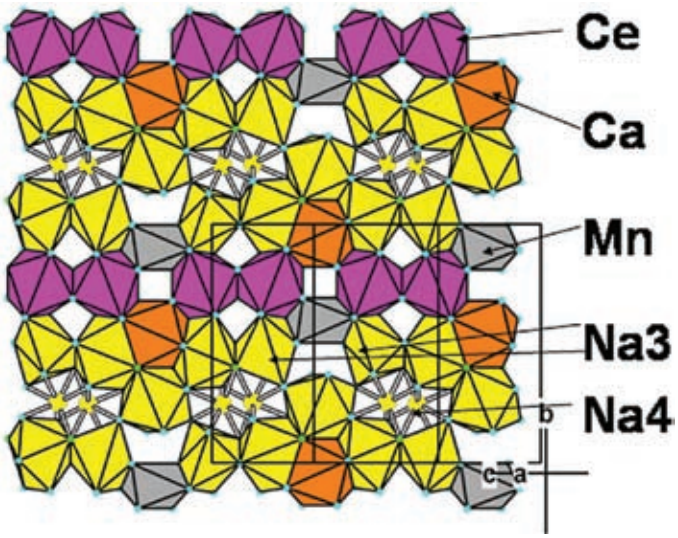

FIG. 7. Large-cation layer in the structure of bussyite-(Ce). The [CeO_8] polyhedra are shown in red, [CaO_8] polyhedra, in orange, [NaO_n] polyhedra, in yellow, and [MnO_6] octahedra, in grey.

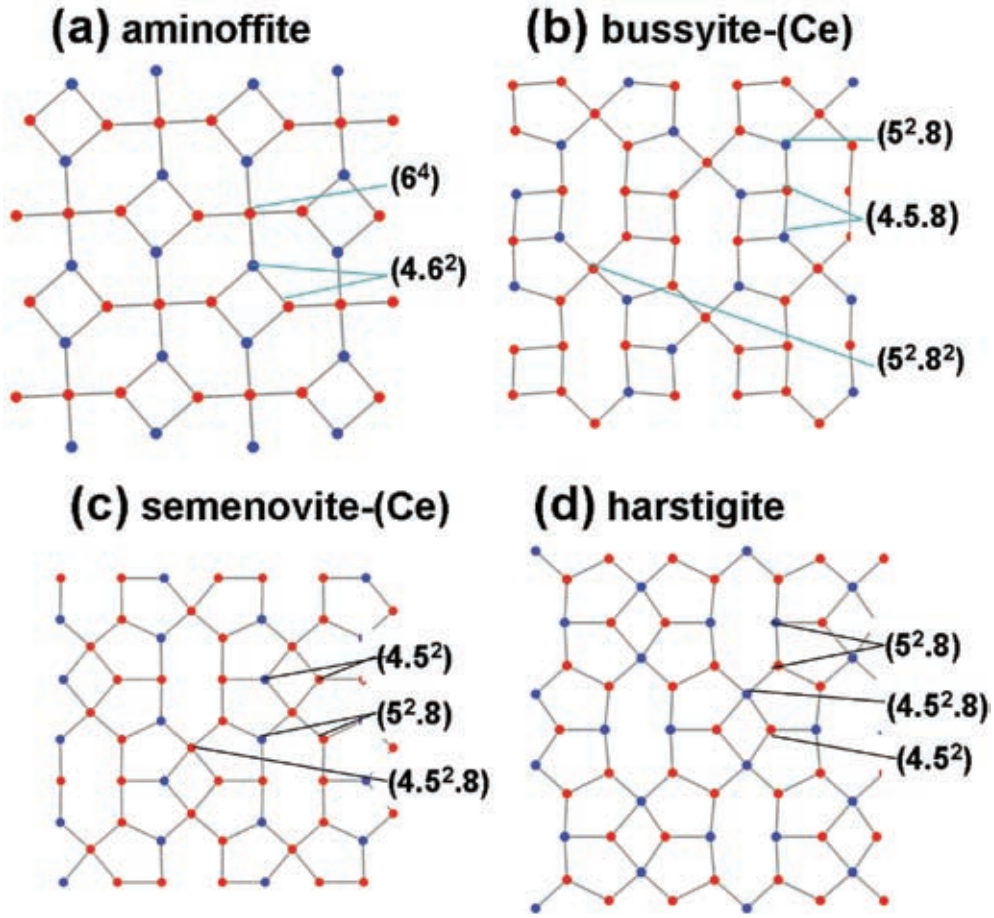

FIG. 8. Topologies of the layers of tetrahedra in selected beryllium silicates. The [SiO_4] tetrahedra are represented by red circles, and the [BeO_4] tetrahedra are represented by blue circles; (a) aminoffite, (b) bussyite-(Ce), c) semenovite-(Ce), (d) harstigite.

ACKNOWLEDGEMENTS

The authors gratefully acknowledge the cooperation of, and samples provided by, Dr. Peter Tarassoff and Mr. Gilles Haineault. The authors thank Dr. Frank C. Hawthorne, University of Manitoba, for the use of his four-circle diffractometer, and Elizabeth Moffatt of the Canadian Conservation Institute for the infrared spectrum. Helpful comments from Drs. Ed Grew and Fernando Cámara as reviewers, Associate Editor Andrew M. McDonald and Editor Robert F. Martin improved the quality of the manuscript.

REFERENCES

BRESE, N.E. & O'KEEFFE, M. (1991): Bond-valence parameters for solids. *Acta Crystallogr*. **B47**, 192-197.

BUSSY, A.B. (1828): Préparation du glucinium. *J. de Chimie Médicale, de Pharmacie et de Toxicologie* **4**, 455-456.

FARMER, V.C. (1974): *The Infrared Spectra of Minerals*. Monograph 4, Mineralogical Society, London, U.K.

GREW, E.S., ed. (2002): Beryllium: Mineralogy, Petrology and Geochemistry. *Rev. Mineral. Geochem.* **50**.

GRICE, J.D. (2008): Berylium silicates: new minerals, structure topologies, classification and uses. *Goldschmidt Conf., Abstr.* **A329**.

GRICE, J.D. & HAWTHORNE, F.C. (2002): New data on meliphanite, $Ca_4(Na,Ca)_4Be_4AlSi_7O_{24}(F,O)_4$. *Can. Mineral.* **40**, 971-980.

HAWTHORNE, F.C. & HUMINICKI, D.M.C. (2002): The crystal chemistry of beryllium. *In* Beryllium: Mineralogy, Petrology and Geochemistry (E.S. Grew, ed.). *Rev. Mineral. Geochem.* **50**, 333-403.

HAWTHORNE, F.C. & SMITH, J.V. (1986): Enumeration of 4-connected 3-dimensional nets and classification of framework silicates. 3-D nets based on insertion of 2-connected vertices into 3-connected plane nets. *Z. Kristallogr.* **175**, 15-30.

HESSE, K.-F. & STÜMPEL, G. (1986): Crystal structure of harstigite, $MnCa_6Be_4[SiO_4]_2[Si_2O_7]_2(OH)_2$. *Z. Kristallogr*. **177**, 143-148.

LIEBAU, F. (1985): *Structural Chemistry of Silicates*. Springer-Verlag, Berlin, Germany.

MAZZI, F., UNGARETTI, L., DAL NEGRO, A., PETERSEN, O.V. & RÖNSBO, J. (1979): The crystal structure of semenovite. *Am. Mineral.* **64**, 202-210.

POUCHOU, J.L. & PICHOIR, F. (1984): A new model for quantitative X-ray microanalysis. I. Application to the analysis of homogeneous samples. *La Recherche Aérospatiale* **3**, 13-38.

RAADE, G. (2008): Beryllium in alkaline rocks and syenitic pegmatites. *Norsk Bergverksmuseums skriftserie* **37**.

SHELDRICK, G.M. (1990): SHELXTL*, a Crystallographic Computing Package* (revision 4.1). Siemens Analytical Instruments, Inc., Madison, Wisconsin.

SHELDRICK, G.M. (1998): SADABS *User Guide*. University of Göttingen, Göttingen, Germany.

SMITH, J.V. (1977): Enumeration of 4-connected 3-dimensional nets and classification of framework silicates. I. Perpendicular linkage from simple hexagonal nets. *Am. Mineral.* **62**, 703-709.

Received May 21, 2008, revised manuscript accepted December 10, 2008.